Received: 19 Feb 2022 | Accepted: 26 Sep 2022 | Available online: 23 Mar 2023
DOI: http://dx.doi.org/10.18180/tecciencia.2022.34.4

TECCIENCIA

UNIVERSIDAD · ECCI

RESEARCH ARTICLE

Engineering

Effect of varying percentages of Co_3O_4 Nanoparticles on the Behavior of (ORR/OER) Bifunctional $Co_3O_4/\alpha - MnO_2$ Electrocatalyst

Efecto de porcentajes variables de nanopartículas de Co_3O_4 en el comportamiento del electrocatalizador bifuncional (ORR/OER) $Co_3O_4/\alpha - MnO2$

Awan Zahoor [1,2] | **Ghadia Ahmed** [3] | **Muhammad Amir** [4] | **Faaz Butt** [5] | **Asad A. Naqvi** [6]

[1]1Department of Polymer Engineering, NED University of Engineering and Technology Karachi, Pakistan

[2]2Department of Food Engineering, NED University of Engineering and Technology, Karachi, Pakistan

[3]Department of Chemical Engineering, NED University of Engineering and Technology, Karachi, Pakistan

[4]Department of Textile Engineering, NED University of Engineering and Technology, Karachi, Pakistan

[5]Department of Materials Engineering, NED University of Engineering and Technology, Karachi, Pakistan

[6]Department of Mechanical Engineering, NED University of Engineering and Technology, Karachi, Pakistan

Correspondence
Awan Zahoor
Email: zahoor@cloud.neduet.edu.pk

Edited by : Angie L. Fula.

How to cite: Awan Zahoor et al., **Effect of varying percentages of Co_3O_4 Nanoparticles on the Behavior of (ORR/OER) Bifunctional $Co_3O_4/\alpha - MnO_2$ Electrocatalyst**, TECCIENCIA, Vol. 18, No. 34, 43-52, 2023
DOI:http://dx.doi.org/10.18180/tecciencia.2022.34.4

Abstract. Among all types of batteries, Lithium Air Batteries (LAB) are considered to be the most effective due to their highest energy density of around 11,140 Wh/kg but there are some major issues that are being faced by LAB such as large overpotential, poor cycle life, low current density, and decreased energy efficiency. The solution to these issues is primarily dependent on the proper selection of an electrocatalyst. A new approach for using a bi-functional electrocatalyst produced excellent results. Here, $Co_3O_4/\alpha - MnO_2$ composite has been considered as a bifunctional catalyst because cobalt oxide performed well in the Oxygen Evolution Reaction (OER) process while manganese oxide performed well in the Oxygen Reduction Reaction (ORR) process. A simple two-step hydrothermal process is used in this work to synthesize $Co_3O_4/\alpha - MnO_2$. This work focuses on the behavior of the composite electrocatalyst when varying percentages of Cobalt oxide (5%, 10%, 15%, and 20%) are deposited on the alpha-Manganese Oxide nanorods. The primary characteristics of each sample with different percentages of Cobalt Oxide are examined, and the performance of each sample is compared to one another. Several testing techniques like Cyclic Voltammetry (CV), Linear Sweep Voltammetry (LSV), X-Ray Diffraction (XRD), and Scanning Electron Microscopy (SEM) are performed on the samples. The combination of cobalt oxide and manganese oxide showed a synergistic effect and work as a bifunctional electrocatalyst. As the percentage of Co_3O_4 deposited on the $\alpha - MnO_2$ nanorod increased, it behaves more like an OER electrocatalyst leading to a decrease in charging potential. This work will help in finding an optimum amount of Co_3O_4 that should be deposited on $\alpha - MnO_2$ nanorods to get an efficient (ORR/OER) bifunctional electrocatalyst.

Keywords: Li-air Batteries, OER/ORR processes, Bifunctional Electrocatalyst, $Co_3O_4/\alpha - MnO_2$ composite

Resumen

Entre todos los tipos de baterías, las de litio-aire (LAB) se consideran las más eficaces debido a su mayor densidad energética, de unos 11.140 Wh/kg, pero las LAB se enfrentan a algunos problemas importantes, como un gran sobrepotencial, una vida útil deficiente, una baja densidad de corriente y una menor eficiencia energética. La solución a estos problemas depende principalmente de la selección adecuada de un electro catalizador. Un nuevo enfoque para utilizar un electrocatalizador bifuncional produjo excelentes resultados. En este caso, se ha considerado el compuesto $Co_3O_4/\alpha - MnO_2$ como catalizador bifuncional, ya que el óxido de cobalto obtuvo buenos resultados en el proceso de Reacción de Evolución de Oxígeno (OER), mientras que el óxido de manganeso obtuvo buenos resultados en el proceso de Reacción de Reducción de Oxígeno (ORR). En este trabajo se utiliza un sencillo proceso hidrotermal de dos pasos para sintetizar $Co_3O_4/\alpha - MnO_2$. Este trabajo se centra en el comportamiento del electrocatalizador compuesto cuando se depositan porcentajes variables de óxido de cobalto (5%, 10%, 15% y 20%) sobre los nanorods de óxido de alfa-manganeso. Se examinan las características primarias de cada muestra con distintos porcentajes de óxido de cobalto y se compara el rendimiento de cada una de ellas entre sí. Las muestras se someten a diversas técnicas de ensayo, como la voltamperometría cíclica (CV), la voltamperometría de barrido lineal (LSV), la difracción de rayos X (DRX) y la microscopía electrónica de barrido (SEM). La combinación de óxido de cobalto y óxido de manganeso mostró un efecto sinérgico y funciona como un electrocatalizador bifuncional. A medida que aumenta el porcentaje de Co_3O_4 depositado sobre el nanorod $\alpha - MnO_2$, éste se comporta más como un electrocatalizador OER dando lugar a una disminución del potencial de carga. Este trabajo ayudará a encontrar la cantidad óptima de Co_3O_4 que debe depositarse sobre los nanorods de $\alpha - MnO_2$ para obtener un electrocatalizador bifuncional (ORR/OER) eficiente.

Palabras clave: Baterías de Li-aire, procesos OER/ORR, electrocatalizador bifuncional, compuesto $Co_3O_4/\alpha - MnO_2$

1 | INTRODUCTION

For many years, fossil fuels have been the primary focus for global energy production and monetary benefits. However, fossil fuels are gradually depleting over time, causing severe environmental damage. As a result of a finite supply of fossil energy resources and severe environmental consequences, the development of renewable and sustainable energy resources is gaining popularity [1]. Renewable resources, on the other hand, are inherently intermittent, necessitating the development of efficient and cost-effective energy storage systems. Because vehicles consume the majority of fossil fuels [1], the primary emphasis should be on an energized transportation system. Electric vehicles (EVs) have made an important contribution to this transportation structure by lowering greenhouse gas emissions and the use of petroleum-derived fuels. Traditional rechargeable batteries are a strong contender for energy storage due to their great energy efficiency and cycle performance. Li-ion batteries are ideal for small energy storage systems because of their long life, high efficiency, high energy density, and low cost. However, Lithium-ion batteries still require a lot of improvement. On the other hand, metal-air batteries are becoming increasingly popular due to their higher theoretical energy density, which is comparable to that of gasoline. Researchers have long considered the use of zinc-air batteries due to their convenience, and long-time span, whereas iron-air batteries have a long-life cycle. However, in comparison to other metal-air batteries, its voltage is low and it has obvious vitality. Aluminum is one of the world's infinite resources and has high vitality thickness [1], which is why aluminum-air batteries are important. In comparison to that of gasoline (13000 Wh/kg [1]), a zinc-air battery has an energy density of only 1084 Wh/kg, which is a significantly lower energy density and insufficient to meet the energy demands of electric vehicles [1], [2], [3], [4], [5].

LAB has recently been suggested as a promising power source that can store a large amount of electrical energy for a long time. Li-air batteries have an energy density of about 11,140 Wh/kg [6] (based on Lithium metal mass), which is comparable to gasoline, and thus are more suitable for electric vehicles than lithium-ion

batteries. Li-air batteries have the highest specific theoretical energy density (3500 to 3600 Wh/kg [7], [8]), accounting for about 20% [8] of the regular Li-ion Batteries making them attractive power source for electric vehicles. LAB is composed of a lithium metal anode, electrolyte, carbon cathode, and an external oxygen source. In a Li-air battery, an oxidation-reduction cycle between lithium metal and air produces an electric current. The LAB is an open cell structure with an infinite external oxygen source and a constant supply of oxygen from the ambient air. The Li-air battery has a higher theoretical vital thickness since oxygen is supplied from outside the battery rather than stored within it [1], [9]. LAB contains a porous carbon cathode from which the O_2 gas is taken in the cell. At the cathode, the O_2 gas, and the electrons and Li+ ions from the electrolyte solution combine to form the insulating material Lithium peroxide (Li_2O_2) as the discharge product [10] as shown in Fig. 1 Resulting in the addition of an electrocatalyst layer for reducing electrode overpotential and a gas-diffusion layer (GDL) for oxygen transport between the surrounding air and the cathodic surface [7]. For the anode part of the cell, a Lithium metal is selected for its high specific capacity (3860 mAh/g) and low redox potential (3.04V versus SHE) [11], [10]. The cathode and anode are immersed in an aprotic Li-ion conducting electrolyte solution.

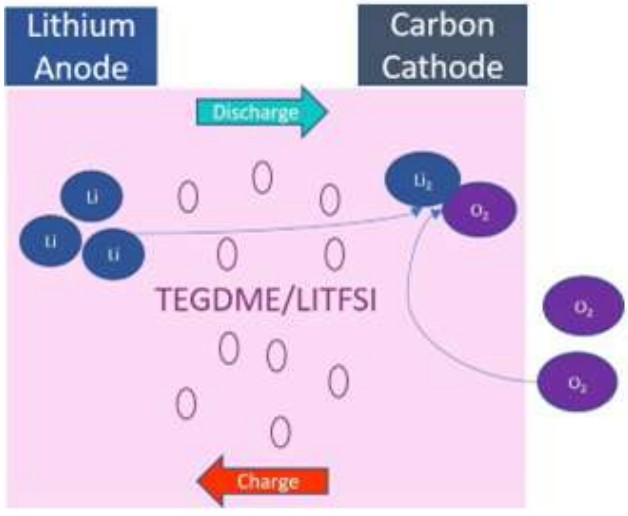

FIG. 1 Schematic Diagram of a Li-air Battery

Aprotic Lithium-Air Batteries have been extensively researched, with the electrochemical reaction of [9], [12]

$$2Li^+ + O_2 + 2e^- \iff Li_2O_2(Discharge/ChargeReaction) \tag{1}$$

Here, the primary focus is on the formation/degradation of discharge product (Li_2O_2). During the oxygen reduction reaction (ORR), Li metal from the anode is electrochemically oxidized to Li+ ions and discharged into the electrolyte, while electrons pass through the external circuit to the cathode. Meanwhile, oxygen is reduced on the porous cathode surface to produce toroid-shaped Li_2O_2. The oxygen supply is impeded by the insulating property of Li_2O_2, which slows interfacial charge transfer [10]. This results in high overpotential, poor cycle life, low current density, and decreased energy efficiency. Usually, these problems are caused by the selection of materials used as an electrocatalyst.

For LAB, a high-performance ORR electrocatalyst is a key requirement. Among the ORR electrocatalysts, noble metals, especially platinum (Pt), perform the best and most promising as cathode material. Pt-based catalysts are not commonly employed in commercial applications because of the high price and scarcity of precious Pt metal. As a result, considerable research efforts should be focused on producing non-Pt-based

new generation ORR catalysts that are both highly efficient and inexpensive [13].

Several other ORR electrocatalysts have been reported in the literature, including non-precious transition metal-based oxides (perovskite [14], spinels and pyrochlore [15], [16], [17] single oxide [18], and multiple oxides [19], [20], MnO_2, $Ni(OH)_2$, and Fe_2O_3, conducting polymers (polyanilines and polythiophenes, etc.), organometallic compounds [21], and carbon-based materials (such as N-doped carbon nanotubes, graphene, and carbon nanofiber) [22] and their composites have been studied [23]. Manganese dioxide has gained popularity as an electrocatalyst for ORR in alkaline electrolytes due to its easy availability, strong catalytic activity, and low price. Spinel Co_3O_4 has also been investigated as an ORR electrocatalyst due to its great catalytic performance. J. Chen et al. [24] reported that CoMn spinel oxides with many defects and vacancies exhibited exceptional electrocatalytic performance in the reduction reaction. As a result, it is expected that the electrocatalytic performance of cobalt and manganese oxides in an alkaline medium will be improved by the use of MnO_2 nanorods modified with Co_3O_4 nanoparticles, which will establish a new class of long-lasting and low-priced ORR electrocatalyst [23]. The interaction between the two metal oxides on the interface is suitable for one-dimensional nanorods as an air electrocatalyst, which offers several advantages such as fast ions mass transport, low mass loading, fast charge transport, and improved mechanical robustness [25]. When Tan et al. developed a hybrid Zn battery composed of a Co_3O_4 network connected with 2-dimensional carbon nanosheets and used it as an active material, it resulted in high battery capacity and long cycle life [26].

On the other hand, a transition metal oxide catalyst MnO_2, has not only been used in supercapacitors [27], [28] but it has also demonstrated exceptional ORR catalytic activity in lithium air batteries [29], [30]. Bruce et al. [31], the catalytic performance of MnO_2 is greatly affected by its crystalline structure. They found that $\alpha - MnO_2$ performs more effectively in comparison to other structures. Li-air batteries with a large $\alpha - MnO_2$ (2x2) tunnel structure can store and remove lithium oxides more reversibly while also promoting rapid diffusion of oxygen and lithium ions, making it an excellent ORR electrocatalyst. Cao et al [32] demonstrated that the catalytic activity of oxygen reduction of $\alpha - MnO_2$ is greater than that of $\beta - MnO_2$, $\lambda - MnO_2$, $\gamma - MnO_2$ and is closer to that of δMnO_2. However, MnO_x has low intrinsic conductivity (e.g., 10^{-5} to 10^{-6}S cm^{-1} for MnO_2) and poor OER kinetics [33], preventing it from being an efficient bifunctional electrocatalyst. In comparison to MnO_2, Co_3O_4 has excellent OER kinetics but mild ORR performance [34]. Furthermore, CoO_x has a high electron conductivity, which makes it a suitable conductive medium for MnO_x [35]. Based on the above analysis, a $Co_3O_4/\alpha - MnO_2$ composite can be assembled to achieve an efficient ORR/OER bifunctional electrocatalyst [35].

This work focuses on the deposition of Co_3O_4 nanoparticles on the tetragonal alpha-phase structured manganese dioxide nanorods via a hydrothermal technique that works as a bifunctional catalyst. Different samples with varying percentages of Co_3O_4 are deposited on $\alpha - MnO_2$ nanorods. Their primary characteristics are examined, and the performance of each ORR electrocatalyst is compared to one another. Several testing techniques like Cyclic Voltammetry (CV), Linear Sweep Voltammetry (LSV), X-Ray Diffraction (XRD), and Scanning Electron Microscopy (SEM) are performed on the samples. The combination of cobalt oxide and manganese oxide showed a synergistic effect. As the percentage of Co_3O_4 deposited on the $\alpha - MnO_2$ nanorod increased, it behaves more of an OER electrocatalyst.

2 | EXPERIMENTAL

2.1 | Chemicals

Cobalt (II) nitrate hexahydrate (98%), ethylene glycol ($\geq 99.5\%$), potassium permanganate ($\geq 99\%$) and potassium hydroxide (0.1 M) were purchased from Sigma-Aldrich.

2.2 | Material Synthesis

$Co_3O_4/\alpha - MnO_2$ nanorods composite materials were prepared via a revised two-step hydrothermal method. $\alpha - MnO_2$ were synthesized in the first step of the hydrothermal method as reported previously [31]. Sub-

sequently, Co_3O_4 particles were deposited on the surface of $\alpha - MnO_2$ nanorods in the second step of the hydrothermal method. First, $\alpha - MnO_2$ (0.2 g) was dissolved in ethylene glycol (100 ml) and sonicated to agitate the particles in the sample by applying sound energy for 30 minutes. Then, for 5% Co_3O_4, $Co(NO_3)_2.6H_2O$ (0.013 g) was dissolved in ethylene glycol (100 ml) and sonicated for 30 minutes. Next, cobalt nitrate solution was added into the MnO_2 solution. The pH value of the mixture was adjusted to 11 by adding a sufficient amount of KOH (0.1 M). For the proper dispersion, sonicated the mixture for another 30 minutes. Reflux at 160^oC for 2 hours. Cooldown and washed with Deionized water. Dried under vacuum at 105^oC overnight. The same procedure was carried out for 10%, 15%, and 20% of Co_3O_4.

2.3 | Structural and chemical characterizations

The surface morphology and crystallographic properties of the synthesized samples were evaluated by Scanning Electron Microscopy (SEM) with energy dispersive X-ray (EDX), and X-ray diffraction technique (XRD).

2.4 | Electrochemical characterization

To evaluate the electrocatalytic activity and performance of $\alpha - MnO_2/Co_3O_4$, cyclic voltammetry (CV), and rotating disk electrode (RDE) techniques were used to obtain ORR polarization curves. A computerized Potentiostat from CH Instruments (model number CHI 760 D) was used to complete the electrochemical studies using a three-electrode configuration. In a typical test, a Hg/HgO-based reference electrode was used along with Pt wire as a counter electrode. Before any electrochemical test, the electrochemical cell was bubbled with oxygen (O_2) for at least an hour. For the preparation of the working electrode for electrochemical measurements, in a typical scheme, the as-prepared $\alpha - MnO_2$ Co_3O_4 powder was mixed with carbon powder (Cabot Vulcan XC-72) at a 3:7 wt:wt ratio to provide reasonable electrical conductivity. 10 mg of as-prepared $a - MnO_2/Co_3O_04$ with carbon powder is dispersed using ultrasonication in 150μL 5 wt.% Nafion-isopropyl alcohol solution. A quantity of 13.5 μL from the prepared suspension was drop casted on a glassy carbon substrate. A rotating disk electrode (RDE) was used to measure the linear sweep voltammetry (LSV) characteristic using a glassy carbon substrate. For the measurements of ORR polarization curves, the LSVs were obtained in 0.1 M KOH saturated with O_2 at a scan rate of $5mVs^{-1}$ at 1600 rpm.

2.5 | Results and Discussion

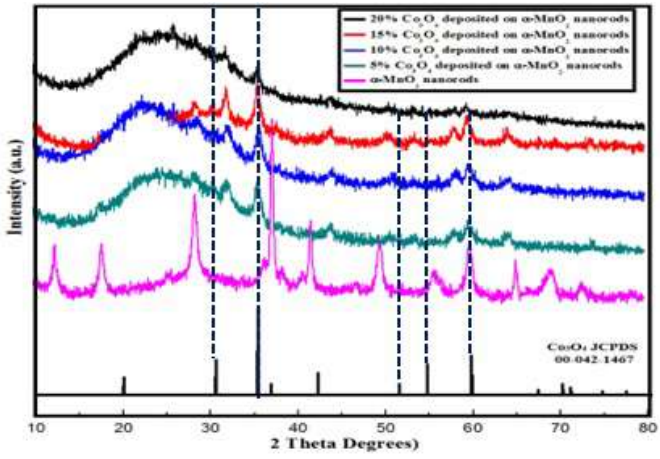

FIG. 2 Theta Degrees. XRD patterns of (Pink) $\alpha - MnO_2$, (Green) 5% $Co_3O_4/\alpha - MnO_2$, (Blue) 10% $Co_3O_4/\alpha - MnO_2$, (Red) 15% $Co_3O_4/\alpha - MnO_2$ and (Black) 20% $Co_3O_4/\alpha - MnO_2$ nanorods, corresponding to JCPDS: 00-042-1467.

Fig. 2 shows the diffraction patterns obtained for the prepared nanomaterials. $\alpha - MnO_2$ nanorods show a crystalline structure with diffraction peaks at 1200, 1039, 2050, 2905, 1530, 1524, and 1309, reflection plane at 12.94^o, 16.88^o, 28.65^o, 37.54^o, 49.87^o, 60.10^o and 65.38^o. There is a peak shift caused by the deposition of Co_3O_4 which results in the disappearance of $\alpha - MnO_2$ peaks, causing the crystalline structure to change into an amorphous structure. 5% Co_3O_4 deposition on $\alpha - MnO_2$ nanorods exhibited the characteristic diffraction peaks at 1336, 1028, reflection plane at 32.13^o, 35.34^o, indicating a slight shift in peaks of $\alpha - MnO_2$ nanorods, beginning to convert into an amorphous structure. The 10% Co_3O_4 deposition exhibited the characteristic diffraction peaks at 1471, 1533, reflection planes at 32.26^o, 35.91^o, indicating further conversion into an amorphous structure. The 15% Co_3O_4 nanorods exhibited the characteristic diffraction peaks at 1643, 1653, and 1197, reflection planes at 32.29^o, 36.01^o, and 59.87^o, representing the coexistence of Co_3O_4 and $\alpha - MnO_2$. The 20% Co_3O_4 (JCPDS: 00-042-1467) nanorods exhibited no or very few peaks of $\alpha - MnO_2$, representing an amorphous structure. The amorphous structure will provide a large Electrochemical surface area (ECSA) to the cathode, as well as high structural flexibility, abundant active sites, and high self-healing capacity, which will improve the overall performance of the Li-Air battery. However, a maximum of 15% Co_3O_4 should be deposited in order to obtain the properties of MnO_2 to promote the ORR reaction in Li-Air batteries.

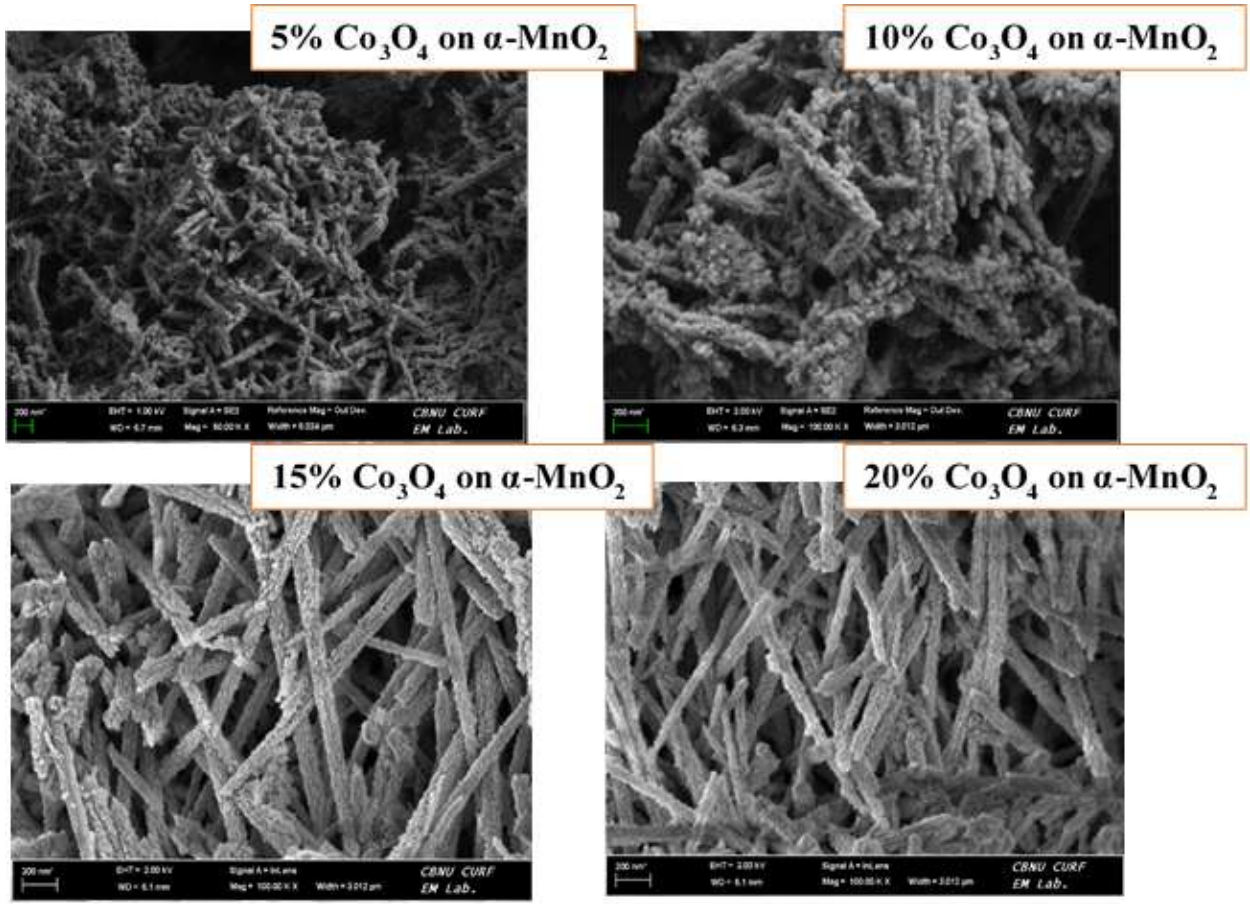

FIG. 3 SEM images of (A) 5% $Co_3O_4/\alpha - MnO_2$, (B) 10% $Co_3O_4/\alpha - MnO_2$, (C) 15% $Co_3O_4/\alpha - MnO_2$ and (D) 20% $Co_3O_4/\alpha - MnO_2$ nanorods.

The morphological properties of the studied nanostructures are evaluated using SEM and the images clearly shows the formation of densely and randomly aligned nanorod structures. The nanorods range in diameter from 80 to 82 nm and have an average length of 1-1.5 m. Fig. 3 (A) depicts a crystalline morphology of $\alpha - MnO_2$ slight deposition of 5% Co_3O_4. When the percentage of Co_3O_4 is increased from 5% to 10% and 15% in (B and C), agglomeration can be seen on $\alpha - MnO_2$ nanorods. (D) shows that 20% Co_3O_4 covers

$\alpha - MnO_2$ nanorods completely with particles ranging in size from 15 to 32 nm. From the SEM image, it can be observed that Co_3O_4 nanoparticles are homogenously distributed over $\alpha - MnO_2$ nanorods, making it less of a bi-functional electrocatalyst.

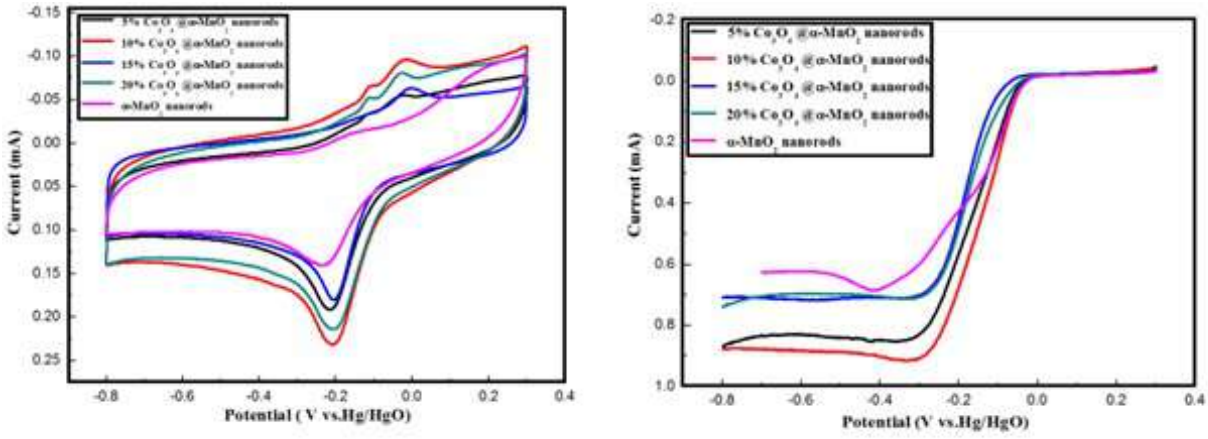

FIG. 4 (left) shows the Cyclic Voltammetry (CV) curves for different samples of $Co_3O_4/\alpha - MnO_2$ in 0.1 M KOH aqueous solution saturated with oxygen at a scan rate of 0.05 V/s. (right) shows the Linear Sweep Voltammetry (LSV) curves for different samples of $Co_3O_4/\alpha - MnO_2$ obtained with RDE at 1600 rpm.

The ORR CV curves for all synthesized samples in 0.1 M KOH aqueous solution saturated with oxygen, at a scan rate of 0.05 V/s, are shown in Fig. 4-left. In Fig. 4-left, oxygen-saturated solutions show quasi rectangular voltammograms when tested for 5%, 10%, 15%, and 20% $Co_3O_4/\alpha - MnO_2$, indicating high surface area carbon. The onset potentials of 5%, 10%, 15%, 20% $Co_3O_4/\alpha - MnO_2$ are -0.08 V, -0.08 V, -0.1 V and -0.07 V, respectively, while it is -0.12 V for $\alpha - MnO_2$. The 20% $Co_3O_4/\alpha - MnO_2$ exhibits a significant positive shift of on-set potential than other samples and $\alpha - MnO_2$. It is clear from the figure that the onset potential of 20% $Co_3O_4/\alpha - MnO_2$ is less negative than other samples and $\alpha - MnO_2$ due to fast reaction kinetics. The peak voltage and peak current for 20% $Co_3O_4/\alpha - MnO_2$ are -0.205 V and 0.217 mA. From this, it can be concluded that 20% $Co_3O_4/\alpha - MnO_2$ is a better performing OER electrocatalyst, due to a positive shift in onset potential and fast reaction kinetics. Fig. 4-right shows the linear sweep voltammetry (LSV) curves obtained with RDE at 1600 rpm to compare ORR electroactivity of MnO_2, 5%, 10%, 15%, and 20% $Co_3O_4/\alpha - MnO_2$. From Fig. 4-right, 20% $Co_3O_4/\alpha - MnO_2$ showed an onset potential of -0.02V with a limiting current of 0.72 mA, while these values are -0.03 V, -0.03 V and -0.05 V for 5%, 10%, 15%, $Co_3O_4/\alpha - MnO_2$ and -0.18 V for $\alpha - MnO_2$ respectively. The half-wave potential for 20% $Co_3O_4/\alpha - MnO_2$ is -0.18 V. LSV curve of 20% $Co_3O_4/\alpha - MnO_2$ presented a much more positive onset potential of 10 mV to 30 mV in comparison with 5%, 10%, 15%, $Co_3O_4/\alpha - MnO_2$, and $\alpha - MnO_2$. The significant positive shift in the 20% $Co_3O_4/\alpha - MnO_2$ relative to 5%, 10%, 15%, $Co_3O_4/\alpha - MnO_2$, and $\alpha - MnO_2$ explicitly shows that 20% $Co_3O_4/\alpha - MnO_2$ is electro-catalytically more active.

3 | CONCLUSIONS

This work focuses on the synthesis of the $Co_3O_4/\alpha - MnO_2$ hybrid via hydrothermal technique. Different samples with varying percentages of Co_3O_4 are deposited on $\alpha - MnO_2$ nanorods. Their primary characteristics are studied, and the performance of each electrocatalyst is compared to one another. Several testing techniques like CV, LSV, XRD, and SEM are performed on the samples. XRD studies show the peak shift of the $\alpha - MnO_2$ nanorods by the deposition of different percentages of Co_3O_4, converting a crystalline structure into amorphous. SEM results show that different percentages of Co_3O_4 agglomerate on $\alpha - MnO_2$ nanorods, resulting in 20% Co_3O_4 with particle sizes ranging from 15 to 32 nm, completely covering the $\alpha - MnO_2$

nanorods. Lastly, Cyclic Voltammetry (CV) and Linear Sweep Voltammetry (LSV) tell the onset potential of every sample, resulting in 20% $Co_3O_4/\alpha - MnO_2$ having a positive shift in onset potential and fast reaction kinetics making it the best performing OER electrocatalyst. This work will open up a new area of research that will find the best optimum amount of Co_3O_4 that should be deposited on an $\alpha - MnO_2$ nanorod in order to obtain the best performance electrocatalyst for both the ORR and OER reactions.

Declaration of Interest

The authors declare that there is no conflict of interest.

References

[1] A. Zahoor, Z. Ghouri, S. Hashmi, F. Raza, S. Ishtiaque, S. Nadeem, I. Ullah, and K. Nahm, "Electrocatalysts for lithium-air batteries: Current status and challenges," *ACS Sustainable Chemistry and Engineering*, vol. 7, p. 14288–14320, 2019. **DOI:** 10.1021/acssuschemeng.8b06351

[2] G. Girishkumar, B. McCloskey, A. C. Luntz, S. Swanson, and W. Wilcke, "Lithium- air battery: promise and challenges," *The Journal of Physical Chemistry Letters*, vol. 1, no. 14, pp. 2193–2203, 2010. **DOI:** 10.1021/jz1005384

[3] Y. Kim, I. Kim, M. Song, and M. Shin, "Poly-vinylidene-fluoride/pbenzoquinone gel polymer electrolyte with good performance by redox mediator effect for li-air battery," *Electrochimica Acta*, vol. 210, p. 821–828, 2016. **DOI:** 10.1016/j.electacta.2016.06.016

[4] K. Surya, M. Michael, and S. Prabaharan, "A review on advancement in non-noble metal based oxides as bifunctional catalysts for rechargeable nonaqueous li/air battery," *Solid State Ionics*, vol. 317, p. 89–96, 2018. **DOI:** 10.1016/j.ssi.2017.12.040

[5] H. Wang and Q. Xu, "Materials design for rechargeable metal-air batteries," *Matter*, vol. 1, p. 565–595, 2019. **DOI:** 10.1016/j.matt.2019.05.008

[6] A. Naqvi, A. Zahoor, A. Shaikh, F. Butt, F. Raza, and I. Ahad, "Aprotic lithium air batteries with oxygen-selective membranes," *Materials for Renewable and Sustainable Energy*, p. 1–14, 2022.

[7] J. Jung, S. Cho, J. Nam, and I. Kim, "Current and future cathode materials for non-aqueous li-air (o2) battery technology – a focused review," *Energy Storage Materials*, vol. 24, p. 512–528, 2020. **DOI:** 10.1016/j.ensm.2019.07.006

[8] A. Laforgue, M. Toupin, A. Mokrini, M. Gauthier, C. Bock, M. Ionescu, B. Luan, X. Yuan, W. Qu, and J. Huot, "Assessment of the li-air battery technology for automotive applications through the development of a multi-electrode solid-state prototype," *EVS 2016 - 29th International Electric Vehicle Symposium*, vol. 8, p. 398–409, 2016.

[9] P. Tan, W. Kong, Z. Shao, M. Liu, and M. Ni, "Advances in modeling and simulation of li–air batteries," *Progress in Energy and Combustion Science*, vol. 62, p. 155–189, 2017. **DOI:** 10.1016/j.pecs.2017.06.001

[10] Y. Zhu, F. Goh, and Q. Wang, "Redox catalysts for aprotic li-o2 batteries: Toward a redox flow system," *Nano Materials Science*, vol. 1, p. 173–183, 2019. **DOI:** 10.1016/j.nanoms.2019.02.008

[11] G. Huang, J. Wang, and X. Zhang, "Electrode protection in high-efficiency li-o2batteries," *ACS Central Science*, vol. 6, p. 2136–2148, 2020. **DOI:** 10.1021/acscentsci.0c01069

[12] S. Yang, P. He, and H. Zhou, "Research progresses on materials and electrode design towards key challenges of li-air batteries," *Energy Storage Materials*, vol. 13, p. 29–48, 2018. **DOI:** 10.1016/j.ensm.2017.12.020

[13] A. Zahoor, R. Faizan, K. Elsaid, S. Hashmi, F. Butt, and Z. Ghouri, "Synthesis and experimental investigation of -mno2/n-rgo nanocomposite for li-o2 batteries applications," *Chemical Engineering Journal Advances*, vol. 7, p. 100115, 2021. **DOI:** 10.1016/j.ceja.2021.100115

[14] V. Neburchilov, H. Wang, J. J. Martin, and W. Qu, "A review on air cathodes for zinc–air fuel cells," *Journal of Power Sources*, vol. 195, no. 5, pp. 1271–1291, 2010. **DOI:** 10.1016/j.jpowsour.2009.08.100

[15] V. Nikolova, P. Iliev, K. Petrov, T. Vitanov, E. Zhecheva, R. Stoyanova, I. Valov, and D. Stoychev, "Electrocatalysts for bifunctional oxygen/air electrodes," *Journal of Power Sources*, vol. 185, p. 727–733, 2008. **DOI:** 10.1016/j.jpowsour.2008.08.031

[16] B. Wang, "Recent development of non-platinum catalysts for oxygen reduction reaction," *Journal of Power Sources*, vol. 152, pp. 1–15, 2005. **DOI:** 10.1016/j.jpowsour.2005.05.098

[17] J. Suntivich, H. Gasteiger, N. Yabuuchi, H. Nakanishi, J. Goodenough, and Y. Shao-Horn, "Design principles for oxygen-reduction activity on perovskite oxide catalysts for fuel cells and metal-air batteries," *Nature Chemistry*, vol. 3, p. 546–550, 2011. **DOI:** 10.1038/nchem.1069

[18] M. Yuasa, M. Nishida, T. Kida, N. Yamazoe, and K. Shimanoe, "Bi-functional oxygen electrodes using lamno3/lanio3 for rechargeable metal-air batteries," *Journal of The Electrochemical Society*, vol. 158, p. 605, 2011. **DOI:** 10.1149/1.3562564

[19] E. Rios, H. Reyes, J. Ortiz, and J. Gautier, "Double channel electrode flow cell application to the study of ho2 ho 2- production on mnxco3-xo 4 (0 x 1) spinel films, electrochimica," *Electrochimica Acta*, vol. 50, 2005.

[20] M. Koninck, S.-C. Poirier, and B. Marsan, "Cu[sub x]co[sub 3x]o[sub 4] used as bifunctional electrocatalyst," *Journal of The Electrochemical Society*, vol. 153, p. 2103, 2006. **DOI:** 10.1149/1.2338631

[21] S. Zhang, Y. Zhao, Z. Yang, Z. He, and H. Wu, "The 1.35 ga diabase sills from the northern north china craton: Implications for breakup of the columbia (nuna) supercontinent," *Earth and Planetary Science Letters*, vol. 288, p. 588–600, 2009. **DOI:** 10.1016/j.epsl.2009.10.023

[22] L. Qu, Y. Liu, J.-B. Baek, and L. Dai, "Nitrogen-doped graphene as efficient metal-free electrocatalyst for oxygen reduction in fuel cells."

[23] C. Cui, G. Du, K. Zhang, T. An, B. Li, X. Liu, and Z. Liu, "Co3o4 nanoparticles anchored in mno2 nanorods as efficient oxygen reduction reaction catalyst for metal-air batteries," *Journal of Alloys and Compounds*, vol. 814, 2020. **DOI:** 10.1016/j.jallcom.2019.152239

[24] F. Cheng, J. Shen, B. Peng, Y. Pan, Z. Tao, and J. Chen, "Rapid room-temperature synthesis of nanocrystalline spinels as oxygen reduction and evolution electrocatalysts," *Nature Chemistry*, vol. 3, p. 79–84, 2011. **DOI:** 10.1038/nchem.931

[25] G. Du, X. Liu, Y. Zong, T. Hor, A. Yu, and Z. Liu, "Co3o4 nanoparticle modified mno2 nanotube bifunctional oxygen cathode catalysts for rechargeable zinc-air batteries," *Nanoscale*, vol. 5, p. 4657–4661, 2013. **DOI:** 10.1039/c3nr00300k

[26] P. Tan, B. Chen, H. Xu, W. Cai, W. He, M. Liu, Z. Shao, and M. Ni, "Co3o4 nanosheets as active material for hybrid zn batteries," *Small*, vol. 14, 2018. **DOI:** 10.1002/smll.201800225

[27] H. Du, C. Wang, and J. Lv, "Controllable morphologies of co3o4@mno2 core-shell structure grown on nickel foam and their supercapacitor behavior," *Solid State Communications*, vol. 277, p. 19–24, 2018. **DOI:** 10.1016/j.ssc.2018.04.009

[28] M. Feng, G. Zhang, Q. Du, L. Su, Z. Ma, X. Qin, and G. Shao, "Co3o4@mno2 core shell arrays on nickel foam with excellent electrochemical performance for aqueous asymmetric supercapacitor," *Ionics*, vol. 23, p. 1637–1643, 2017. **DOI:** 10.1007/s11581-017-2013-1

[29] K. Jung, A. Riaz, S. Lee, T. Lim, S. Park, R. Song, S. Yoon, K. Shin, and J. Lee, "Urchin-like -mno2 decorated with au and pd as a bi-functional catalyst for rechargeable lithium-oxygen batteries," *Journal of Power Sources*, vol. 244, p. 328–335, 2013. **DOI:** 10.1016/j.jpowsour.2013.01.028

[30] P. Zhang, M. He, S. Xu, and X. Yan, "The controlled growth of porous -mno2 nanosheets on carbon fibers as a bi-functional catalyst for rechargeable lithium-oxygen batteries," *Journal of Materials Chemistry A*, vol. 3, p. 10811–10818, 2015. **DOI:** 10.1039/c5ta00619h

[31] A. Débart, A. J. Paterson, J. Bao, and P. G. Bruce, "α-mno2 nanowires: a catalyst for the o2 electrode in rechargeable lithium batteries," *Angewandte Chemie International Edition*, vol. 47, no. 24, pp. 4521–4524, 2008.

[32] Y. Cao, H. Yang, X. Ai, and L. Xiao, "The mechanism of oxygen reduction on mno2-catalyzed air cathode in alkaline solution," *Journal of Electroanalytical Chemistry*, vol. 557, p. 127–134, 2003. **DOI:** 10.1016/S0022-0728(03)00355-3

[33] D. Kong, J. Luo, Y. Wang, W. Ren, T. Yu, Y. Luo, Y. Yang, and C. Cheng, "Three-dimensional co3o4@mno2 hierarchical nanoneedle arrays," *Morphology control and electrochemical energy storage, Advanced Functional Materials*, vol. 24, p. 3815–3826, 2014. **DOI:** 10.1002/adfm.201304206

[34] K. Song, E. Cho, and Y.-M. Kang, "Morphology and active-site engineering for stable round-trip efficiency li–o2 batteries: a search for the most active catalytic site in co3o4," *ACS Catalysis*, vol. 5, no. 9, pp. 5116–5122, 2015.

[35] X. Han, F. Cheng, C. Chen, F. Li, and J. Chen, "A co 3 o 4@ mno 2/ni nanocomposite as a carbon-and binder-free cathode for rechargeable li–o 2 batteries," *Inorganic Chemistry Frontiers*, vol. 3, no. 6, pp. 866–871, 2016.